



Fragmentation and Deuteration in Massive Star Forming Regions



Javier A. Rodón
ESO Santiago, Chile

Henrik Beuther
MPIA Heidelberg, Germany

Peter Schilke
Uni Köln, Germany

Qizhou Zhang
CfA Cambridge, MA, USA

jrodon@eso.org

Motivation

In the last decade, we have started to spatially resolve the relatively small gas and dust condensations in high-mass star-forming regions that will eventually become a massive star or system. We call these condensations of sizes on the order of 0.01 pc "cores", and by estimating their masses we can construct the so-called Core Mass Function (CMF) of a region, to compare with the IMF and try to determine the evolutionary process from core to star.

For massive star-forming regions, the relationship between the CMF and the IMF is not yet well understood. This is, among other factors, due to the fact that there are not many massive CMF determined. Even then, some of those few CMF seem to tell a story of evolution, by presenting different slopes than that of the Salpeter IMF while others, seem to be very similar to the IMF.

But are we in fact observing regions at different evolutionary stages?

Based on the work of Fontani et al. 2011, one way to address this would be by determining the deuterated fraction of those regions, since deuterated species are first released into the gas medium and then destroyed at the early stages of evolution. In this work we show CMFs and deuteration obtained for a group of massive star-forming regions with SMA, PdBI, and IRAM-30m observations. The CMFs show different slopes, while the deuterated fractions found are $\sim 10^4$ times that of the ISM.

The sample and observations

➤ All regions show signs of massive star-formation, are at similar distances (~ 2 kpc), and have similar luminosities ($\sim 10^4 L_{\text{sun}}$). In all cases the cores were identified by eye.

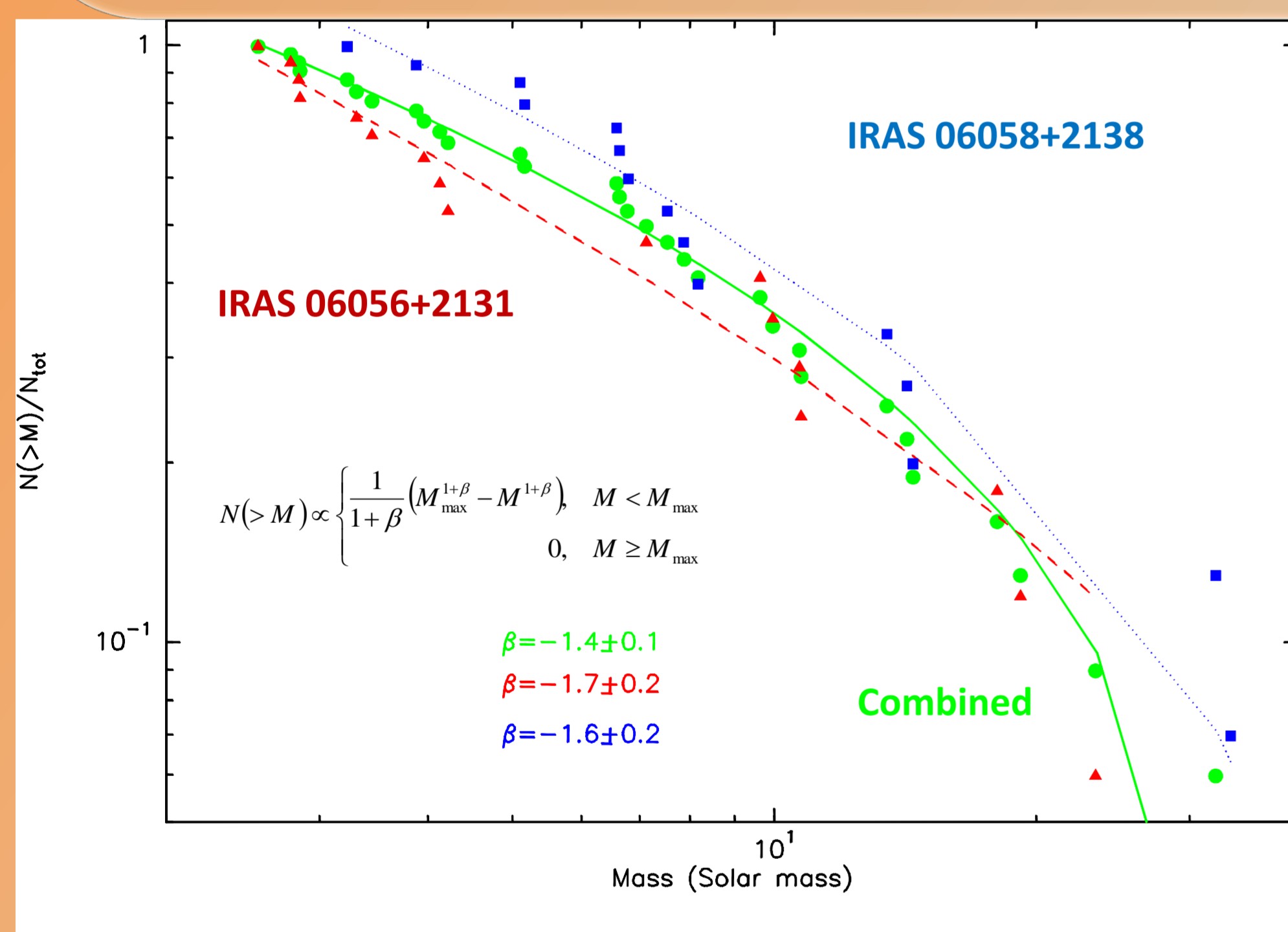
➤ All single-dish molecular line observations shown here were taken with the IRAM 30m telescope.

➤ IRAS 06056+2131: Observed at 1.4 mm with the SMA, we detect 21 cores within two subregions (north and south). Shows a filamentary distribution.

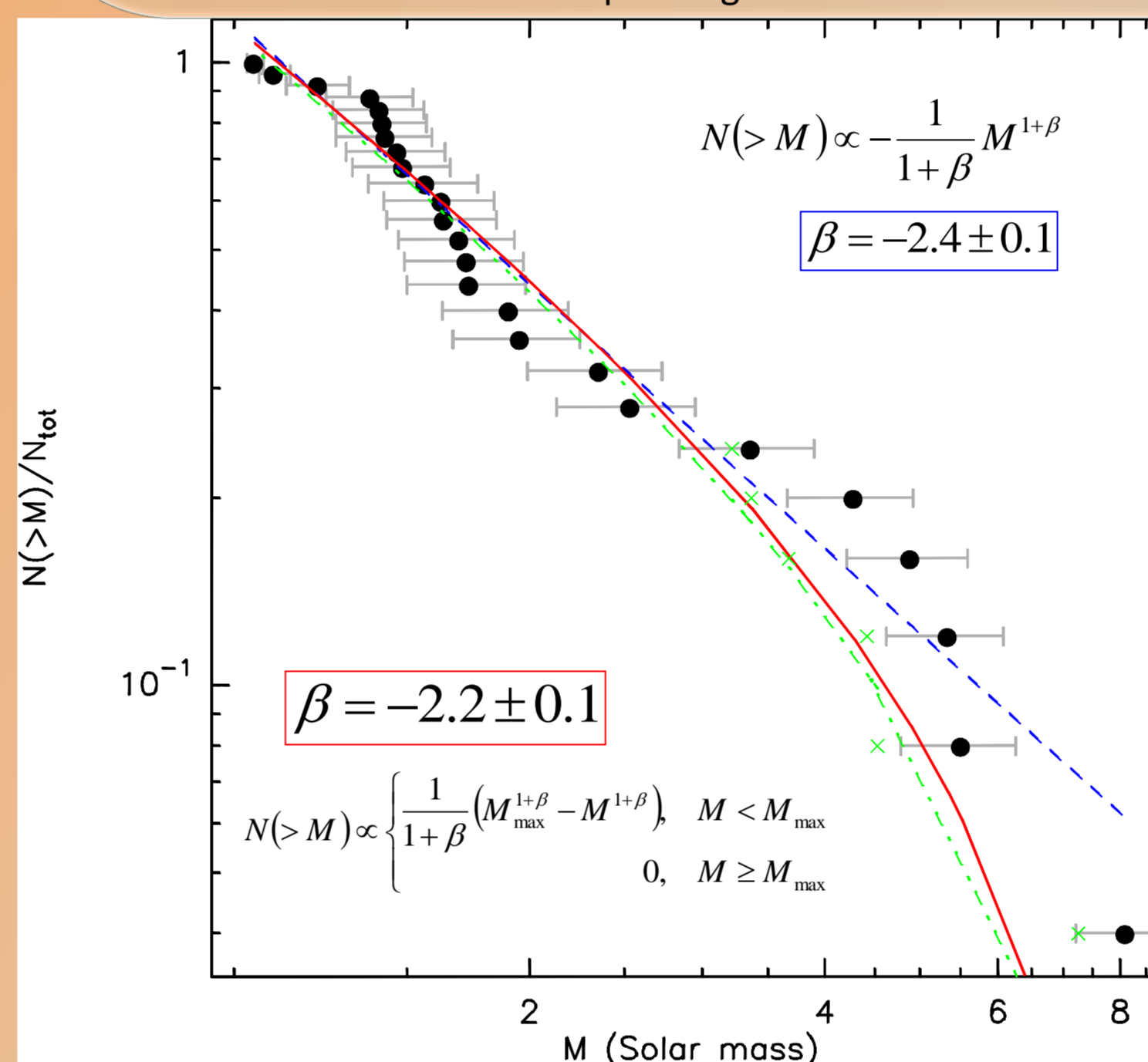
➤ IRAS 06058+2138: Observed at 1.4 mm with the SMA, we detect 15 cores, most of them in a single cluster, with some isolated.

➤ IRAS 19410+2336: Observed at 1.4 mm and 3 mm with the PdBI. We detect 30 cores, with 4 of them detected only at 3 mm. The cores are distributed in two subregions (north and south), both of them with a clustered distribution.

Comparison between the cumulative CMFs of regions IRAS 06056+2131 (red triangles), IRAS 06058+2138 (blue squares), and the cumulative CMF of the combined sample (green circles). The solid, dashed and dotted lines are the best fit to the power law taking into account the upper mass cutoff. The different slopes and their standard deviations are shown in the same color code



Cumulative CMF of IRAS 19410+2336. The solid red line and the dashed blue line represent the best fits of the power law taking into account the upper mass cutoff or not, respectively. The green crosses represent a slight increase of 10K in the higher-mass end, and the green dash-dotted line is the corresponding new fit.



The Core Mass Function

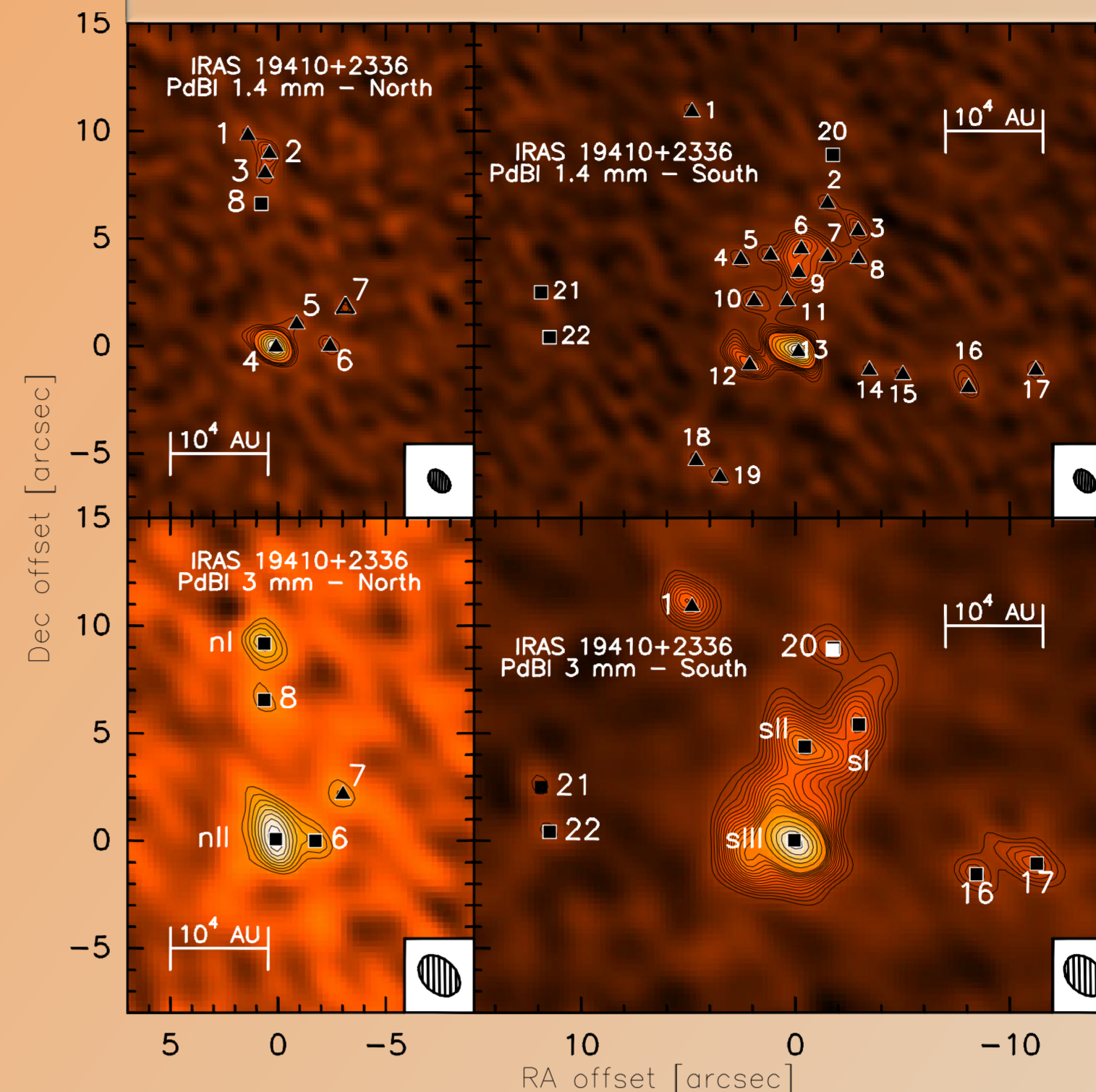
➤ We constructed the cumulative Core Mass Function (CMF) of each region, with masses from dust continuum.

➤ IRAS 06056+2131: Has a CMF slope $\beta = -1.7 \pm 0.2$, flatter than Salpeter.

➤ IRAS 06058+2138: Has a CMF slope $\beta = -1.6 \pm 0.2$, similar to IRAS 06056+2131.

➤ IRAS 19410+2336: Has a CMF slope $\beta = -2.2 \pm 0.1$, similar to Salpeter.

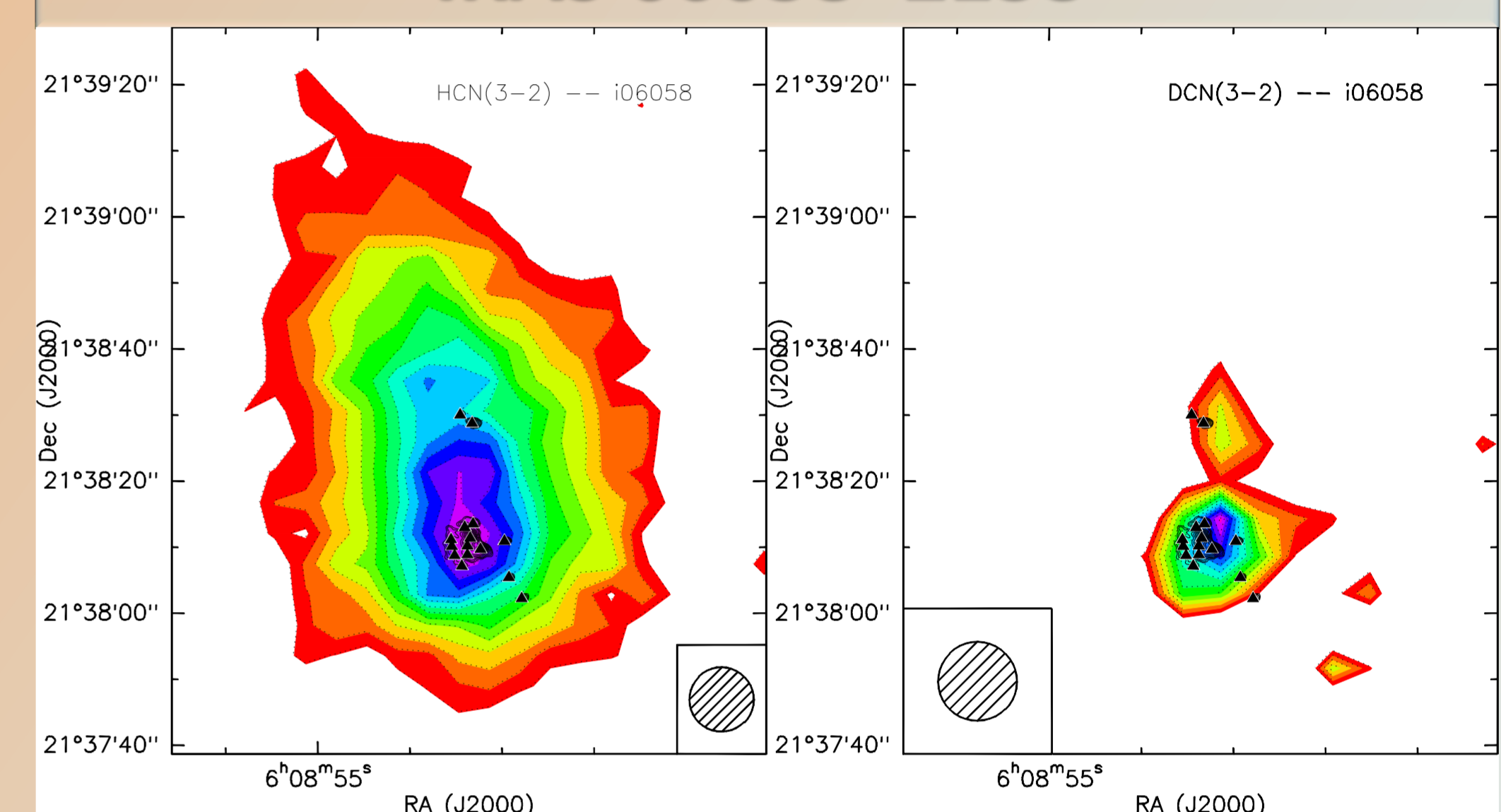
IRAS 19410+2336



Continuum maps of IRAS 19410+2336 obtained with the PdBI. In the top row are the 1.4mm maps of the northern and southern (proto)clusters. Similarly, in the bottom row are the 3mm maps of the northern and southern (proto)clusters. Contours start at 4σ level in all panels.

The triangles mark the position of the sources detected at 1.4 mm, while the squares are the sources detected at 3 mm. A square appearing in a 1.4mm map indicates a source that is only detected at 3 mm. Similarly, a triangle in a 3mm map signals a source detected at the same position in a 1.4mm map.

IRAS 06058+2138



HCN(3-2) map: contouring starts at 5σ and increases in $2\sigma = 1.7$ K.km/s steps. The peak is $S \sim 26$ K.km/s.

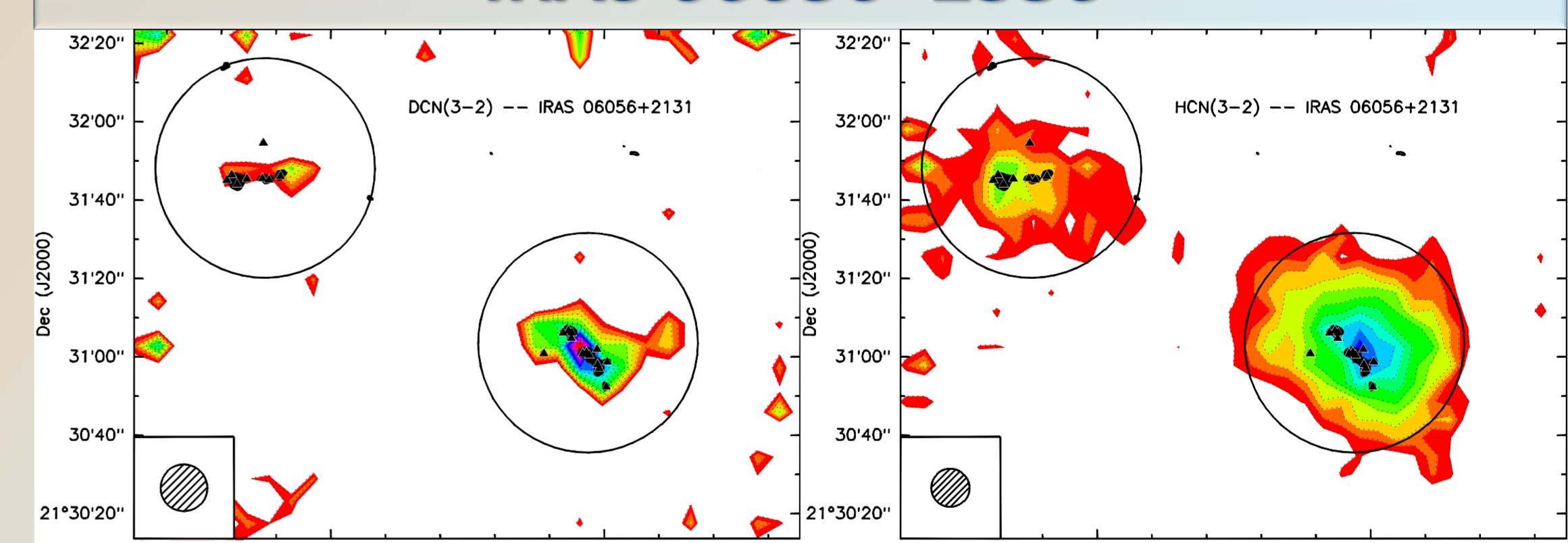
DCN(3-2) map: contouring starts at 5σ and increases in $1\sigma = 0.12$ K.km/s steps. The peak is $S \sim 2$ K.km/s.

❖ The HCN/DCN pair peak at the central cluster, though DCN peaks towards the border of the continuum emission and HCN matches the continuum peak.

❖ The secondary northern peak in both DCN/HCN is likely associated with the parental cloud of the 2 northern mm sources.

❖ HCN is more extended than both D-bearing species, as well as stronger. This reflects on the relatively advanced stage of evolution of this region (NIR sources and masers detected).

IRAS 06056+2336



HCN(3-2): contouring starts at 3σ and increases in $1\sigma = 1.2$ K.km/s steps.

DCN(3-2): contouring starts at 6σ and increases in $1\sigma = 0.1$ K.km/s steps.

Black solid contours are the 1.4mm continuum emission, and the triangles mark the cores identified.

❖ The HCN/DCN pair in the south behave as for the previous region, with DCN peaking to one side of the continuum emission and HCN towards it. In the north, however, both peak to a side of the continuum.

❖ DCN in the south show peaks not associated with the continuum emission, not seen in HCN. Possibly young and cold clumps.

Deuterated fraction [D/H]

➤ We obtained the deuterated fraction [D/H] from the DCN(3-2) and HCN(3-2) observations of the regions.

➤ As a first approximation, we integrated over a single beam towards the continuum emission peaks.

➤ The column densities were calculated with MADCUBA_IJ and CLASS

Source	Species				[D/H]
	DCN		HCN		
	I (K.km/s)	log N (cm ⁻²)	I (K.km/s)	log N (cm ⁻²)	
i19410	1.41	12.14	6.72	12.75	0.25
i06058	1.61	12.05	9.07	12.88	0.15
i06065n	0.86	11.92	3.39	12.45	0.30
i06065s	1.04	12.01	5.17	12.64	0.23

Results

❖ Several theories could explain the difference between the slopes of the CMFs. One possibility, for example, is that we are looking at regions at different evolutionary stage. In any case, with the data we currently have we cannot conclusively determine a reason for why the slope is flatter than Salpeter in one case, but similar to it in another.

❖ A Salpeter-like CMF would suggest a one-to-one core-star relationship, while a flatter slope would suggest further processing between fragmentation and the final formation stage.

❖ Observations at high-angular resolution of similar regions, and numerical simulations of the fragmentation process can and should be done to obtain an explanation.

❖ One way to estimate the evolutionary stage is with the deuterated fraction [D/H], with lower ratios for more evolved regions, i.e., according to our hypothesis, flatter slopes. With only three [slope;D/H] pairs so far, we can hardly observe any correlation in our data. We will continue to gather data on similar regions.

❖ The [D/H] factors obtained are ~ 4 orders of magnitude higher than the standard ISM value of $\sim 10^{-5}$, and are characteristic of high-mass starless core candidates. We believe this is reflecting the fact that we are tracing the clump, and not the individual cores. Observations with better angular resolution are needed to address this fact.

References:

- H. Beuther & P. Schilke, 2004, Science
- F. Fontani et al., 2011, A&A
- R. Klein et al., 2005, ApJS
- J.A. Rodón, 2009, PhD thesis
- J.A. Rodón, H. Beuther, P. Schilke, 2012, A&A
- J.A. Rodón, H. Beuther, Q. Zhang, 2013, A&A in prep.
- MADCUBA_IJ
- http://cab.inta-csic.es/madcuba/MADCUBA_IMAGEJ/ImageJMadcuba.html

